

VAP-PLGA microspheres (VAP-PLGA) promote adipose-derived stem cells (ADSCs)-induced wound healing in chronic skin ulcers in mice via PI3K/Akt/HIF-1 α pathway

Wen Jiang^{a,*}, Jun Zhang^{b,*}, Xudong Zhang^c, Chenghong Fan^d, and Jinlong Huang^{id}^b

^aFirst Clinical School Medicine, Nanjing University of Chinese Medicine, Nanjing City, China; ^bDepartment of Plastic Surgery, Affiliated Hospital Nanjing University of Chinese Medicine, Nanjing City, China; ^cDepartment of Aesthetic and Plastic Surgery, 903RD Hospital of PLA, Hangzhou City, China; ^dAesthetic Surgery Department, Lishui Fan Chenghong Medical Aesthetic Clinic, Lishui City, China

ABSTRACT

Chronic skin ulcers are a primary global health problem. Velvet antler polypeptide (VAP) regulates endothelial cell migration and angiogenic sprout. Adipose-derived stem cells (ADSCs) are reported to make pivotal impacts upon wound healing. This study aimed to explore the role of VAP combined with ADSCs in wound healing of chronic skin ulcers. The effect of VAP on phenotypes of ADSCs, and VAP (PLGA microspheres) combining with ADSCs on wound healing of chronic skin ulcers *in vivo* was evaluated. VAP generally promoted the proliferation, migration and invasion of ADSCs, and ADSC-induced angiogenesis in human umbilical vein endothelial cells (HUVECs) through PI3K/Akt/HIF-1 α pathway. VAP-PLGA (PLGA microspheres) enhanced the promoting effect of ADSCs on wound healing, pathological changes, and angiogenesis in chronic skin ulcers *in vivo*. VAP-PLGA intensified the effect of ADSCs on up-regulating the levels of p-PI3K/PI3K, p-Akt/Akt, HIF-1 α , vascular endothelial growth factor (VEGF), stromal cell-derived factor-1 (SDF-1), C-X-C motif chemokine receptor 4 (CXCR4), angiopoietin-4 (Ang-4), VEGF receptor (VEGFR), and transforming growth factor- β 1 (TGF- β 1), and down-regulating the levels of interleukin-1 β (IL-1 β), IL-18 and IL-6 in wound tissues in chronic skin ulcers *in vivo*. Collectively, VAP promoted the growth, migration, invasion, and angiogenesis of ADSCs through activating PI3K/Akt/HIF-1 α pathway, and VAP-PLGA enhanced the function of ADSCs in promoting wound healing *in vivo*, which was associated with angiogenesis, inflammation inhibition, and dermal collagen synthesis.

ARTICLE HISTORY

Received 17 June 2021
Revised 1 October 2021
Accepted 2 October 2021

KEYWORDS


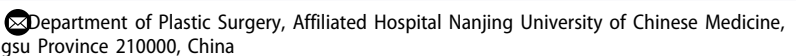
Adipose-derived stem cells (ADSCs); VAP-PLGA microspheres (VAP-PLGA); chronic skin ulcers; wound healing; PI3K/Akt/Hif-1 α pathway

Introduction


Recent years have witnessed the development of chronic skin ulcers including venous leg ulcers, pressure sores and diabetic ulcers into a primary global health problem, initially appearing in the lower extremities, especially in the elderly [1]. Traditional Chinese Medicine (TCM) science categorizes ‘sore and ulcer’ into three syndromes as following: Yang syndrome, Yin syndrome (dull skin, stasis, coldness, and numbness), and semi-Yin and semi-Yang syndrome [2]. Chronic skin ulcers are considered to belong to Yin syndrome (a term in traditional Chinese medicine) skin ulcers [3]. Cutaneous wound repair is associated with a series of biological and molecular processes such as cell migration and proliferation,

extracellular matrix deposition, and remodeling [4]. Growth factors can participate in tissue repair, and those released from the injured site can drive the proliferation and migration of associated cells which are particularly important to wound repair [5].

Given the benefits of natural products, much attention has been focused on traditional and local medicines. Cyclic replacement of deer antlers requires rapid regenerative growth, which, in many ways, is similar to the tissue regeneration process [6]. Velvet antler is one of the most important traditional Chinese medicine from animals with a history of more than 2,000 years, having a wide variety of functions, such as tissue repair

CONTACT Jinlong Huang  huangjinlong_ljh@163.com 

*These authors contributed equally to this work.

 Supplemental data for this article can be accessed [here](#).

© 2021 The Author(s). Published by Informa UK Limited, trading as Taylor & Francis Group.

This is an Open Access article distributed under the terms of the Creative Commons Attribution-NonCommercial License (<http://creativecommons.org/licenses/by-nc/4.0/>), which permits unrestricted non-commercial use, distribution, and reproduction in any medium, provided the original work is properly cited.

[7] and promotion of wound healing [8]. Chronic refractory skin ulcer can be effectively treated with huiyang shengji ointment that consists of velvet antler, *panax*, *Cinnamomum cassia*, *Ligusticum wallichii* and so on [9]. Velvet antler possesses multiple active components including amino acids, polypeptides, and proteins [10], among which velvet antler polypeptide (VAP) is the major bioactive component of velvet antler [11], exerting various health-promoting effects, such as anti-inflammation [12]. The VAP-chitosan-honey suspension could apparently promote the healing of decubitus ulcer [13]. Besides, Guan et al. [14] reported that VAP isolated from the velvet antler of sika deer can stimulate the proliferation of certain cells. Adipose-derived stem cells (ADSCs), similar to other marrow mesenchymal stem cells (MSCs) such as bone marrow-derived MSCs that can express akin markers of MSCs and have self-renewal ability, can also differentiate to various cells such as adipocytes, osteocytes, chondrocytes and myogenic cells with specific culture in different media [15]. The minimum criteria of MSCs include the expressions of CD105, CD73, and CD90, but exclude the expression of CD45, CD34, CD14, or CD11b [16,17]. ADSCs have great differentiation potential and play a critical role in wound healing [18]. Engrafted ADSCs can result in the release of proangiogenic cytokines and factors to enhance repair and regeneration by interacting with local tissues [19].

The PI3K/Akt signaling pathway is instrumental in cancer progression and also indispensable for signal transduction in normal cells [20], which also generates critical effects in many cell functions, such as metabolism, proliferation, migration, invasion, and angiogenesis [21]. Recent studies have demonstrated that PI3K/Akt signaling pathway participates in wound healing *in vivo* [22–26] and exerts a regulatory role in ADSCs during wound healing [27]. Zhang *et al.* [28] also suggest that ADSCs are likely to promote wound healing by releasing exosomes, which may involve PI3K/Akt pathway. Moreover, velvet antler proteins regulate the PI3K/Akt signaling pathway to ameliorate injured cardiac microvascular endothelial cells [29]. Several studies have proved that some gene products, referring to stromal products that include hypoxia and inflammatory intermediates,

can mimic the cytoprotective effects of hypoxia, and stimulate the overexpression of HIF-1 α and other signaling pathways [30,31]. HIF-1 α activates the transcription of diverse genes encoding angiogenic cytokines such as vascular endothelial growth factor (VEGF) [32]. Metabolic reprogramming by HIF-1 α activation enhances survivability of human ADSCs in ischemic microenvironments [33]. Angiopoietin (Ang), VEGF, and C-X-C motif chemokine receptor 4 (CXCR4) are examples of HIF-1 α target genes, which have important roles in stem cell viability, proliferation, and migration [34,35]. Besides, VEGF, a family of angiopoietins (Angs), is another factor that is involved in angiogenesis. Ang 4 has a stimulatory effect on the endothelial cell migration and capillary formation [36,37]. Therefore, it is imperative to fathom out the role of PI3K/Akt/HIF-1 α pathway in the function of VAP and ADSCs in wound healing.

Following that literature review, we hypothesized that VAP promotes the proliferation and migration of ADSCs, and PI3K/Akt/HIF-1 α pathway plays an important part in the roles of VAP and ADSCs on wound healing. In the present study, we intended to investigate the effect and potential mechanism of VAP on the proliferation and migration of ADSCs, so as to understand its stimulating effect on ADSCs. Moreover, we established a skin ulcer model with Yin syndrome *in vivo* to explore whether VAP-PLGA microspheres (VAP-PLGA, one long-acting slow-release dosage form) can improve ADSCs-induced wound healing in chronic skin ulcers. Our objective was to develop combination therapy with ADSCs and VAP-PLGA to improve wound healing during chronic skin ulcers.

Materials and methods

Ethics statement

The animal experiments were performed according to the guidelines of China Council on Animal Care and Use. This research was approved by the Committee of Experimental Animals of Nanjing University of Chinese Medicine (approval number: NM20190720201). Every effort was made to minimize suffering and discomfort of the animals. All

animal experiments were performed in Nanjing University of Chinese Medicine.

ADSC preparation

ADSCs were isolated from subcutaneous adipose tissues of male Kunming (KM) mice, based on previous protocol [19]. In brief, subcutaneous adipose tissues (20–40 mL) obtained by sterile surgical excision were placed into DMEM/F12 (D6421, Sigma), and then washed with phosphate buffered saline (PBS) containing 1% Penicillin-Streptomycin Liquid (P1400, Solarbio, Beijing, China) until no red color remained. Next, after the connective tissues and blood vessels were removed from the adipose tissues with ophthalmic scissors and eye forceps, the adipose tissues were cut into small fragments (1 mm³). Since Collagenase type I digestion solution (0.1%, 17100017, Invitrogen) was dissolved in DMEM, an equal amount of the solution was used to digest the adipose tissues at 37°C for 45–60 min until the tissues were changed into paste. The digestion reaction was stopped using DMEM/F12 containing 10% fetal bovine serum (FBS). The undigested tissues were removed by filtering through a 100-mesh screen, with 150 µm pore diameter. Next, the adipose tissues underwent centrifugation at 1,200 r/min for 10 min. Following that, the supernatant was discarded, while the pellet was collected and resuspended in conditioned medium (DMEM/F12, 10% FBS, 2 ng/mL bFGF, 1% penicillin-streptomycin liquid) and then plated into 6-well plates in an incubator containing 5% CO₂ at 37°C. The medium was changed every 2 days. When the confluence reached 80–90%, the primary ADSCs (P1 ADSCs) were obtained, and then sub-cultured and passaged in conditioned medium at a ratio of 1:3 until the third passage (P3 ADSCs). The cell morphology of P1 and P3 ADSCs was observed under a 200 × inverted microscope (IX71; Olympus, Tokyo, Japan).

Flow cytometry for cell phenotype detection

Cell phenotype detection was performed as previously reported [38]. After reaching 80–90% confluence, P3 ADSCs were digested with 0.25% pancreatin-0.02% ethylenediamine tetraacetic acid

(EDTA; T1300, Solarbio), and then no less than 2×10^5 cells were collected from each sample for analysis. Next, cells were resuspended in 100 µL of PBS and subjected to centrifugation at 1,000 r/min for 5 min. After removing the PBS, cells were resuspended in 200 µL of PBS, incubated for 30 min with antibodies, and washed twice with PBS. After removing the PBS again and resuspending the cells with 300 µL PBS, the cell suspension was analyzed by flow cytometry (Accuri™ C6, BD Biosciences, USA). The following monoclonal antibodies used in this experiment were purchased from eBioscience™ of Thermo Fisher Scientific: anti-CD29-FITC (#11-0291-80), anti-CD90-FITC (#11-0909-42), anti-CD73-FITC (#11-0739-41), anti-CD105-FITC (#MA1-19594), anti-CD34-FITC (#11-0349-41), and anti-CD45-FITC (#11-9459-41) antibodies.

Velvet antler peptides (VAP)

Fresh velvet antlers from Deer Shuangyang district of deer products of heng distribution (<http://www.hengdaluye.com/index.html>) were cut into small pieces, dissolved in HAC-NaAc buffer solution (pH 3.5) at a ratio of 1:5, and then subjected to centrifugation at $8,000 \times g$ for 20 min. The supernatant was collected and then added with ethanol (95%) until the final concentration of 65% was reached. The solution was stirred at 4°C for 4 h, and then centrifuged at $8,000 \times g$ for 20 min. After that, the supernatant was harvested and subjected to rotary evaporation under vacuum at 55°C to evaporate off the ethanol, and then the concentrated solution was obtained. During the freeze-drying process, dried velvet antler peptides powder was acquired from the concentrated peptides. Lastly, the Kjeldahl method was applied to determine the purity of peptides.

Cell treatments

To determine the effect of VAP on ADSCs, ADSCs were treated with VAP at different concentrations (0, 6, 12, 25, and 50 µg/mL). To figure out the roles of PI3K/Akt and HIF-1α signaling in ADSCs, ADSCs were divided into four groups as follows: Control, VAP, VAP+LY294002 and VAP + Perifosine groups. Control group: cells received

no treatment; VAP group: cells were treated with 25 µg/mL VAP; VAP+LY294002 group: cells were pre-treated with 30 µM LY294002 (PI3K family specific inhibitor, 19–142, Sigma-Aldrich) [19] for 2 h, and then treated with 25 µg/mL VAP for an indicated time; VAP + Perifosine group: cells were pre-treated with 10 µM perifosine (Akt-specific inhibitor, SC0227, Beyotime) for 2 h, and then treated with 25 µg/mL VAP for an indicated time.

Cell viability assay

Cell viability was determined by Cell Counting Kit-8 (CCK-8). CCK-8 assay was performed using a CCK-8 kit (CA1210, Solarbio). In short, P3 ADSCs (2,000 cells/well) plated into 96-well plates (100 µL/well) were pre-treated with or without LY294002 or perifosine for 2 h, and then further treated with VAP. After 48 h of culture, 10 µL of CCK-8 solution was added into each well and further incubated for 3 h. Cell viability was determined by measuring the absorbance at 450 nm using a Microplate reader (Tecan, Switzerland).

Cell colony formation assay

The colony formation rate of cell proliferation was determined by colony formation assay. Briefly, ADSCs (1×10^3 cells/well) were cultured in 6-well plates. Conditioned medium was changed every 4 days. Following two weeks of culture, the cells were fixed with 10% methanol for 15 min and then dyed with Crystal Violet Staining Solution (C0121, Beyotime) for 30 min. The number of colonies with over 50 cells was calculated under an inverted microscope (IX71; Olympus, Tokyo, Japan).

Scratch wound healing assay

The migration ability of ADSCs was evaluated by scratch wound healing assay. Briefly, ADSCs were plated in 24-well plates and cultured to reach 90% confluence. Next, the cells were cultured in FBS-free DMEM/F12 overnight. Then, a scratch was created in the cell monolayer using a 10 µL pipette tip and FBS-free DMEM/F12 was replaced by conditioned medium. The images were taken at 0 h under a 100 × inverted

microscope (IX71; Olympus, Tokyo, Japan). Afterward, the cells were pre-treated with or without LY294002 or perifosine for 2 h, and then further treated with VAP for 48 h. After that, images were photographed again by the same method. Finally, the cell migration rate was determined by calculating the reduced breadth of the scratch in ADSCs.

Transwell assay

Cell invasion was performed in transwell chambers (8 µm pores, Corning Inc., Corning, USA) coated with 20 µL of Matrigel. Cells (1.5×10^5) were incubated in 100 µL of FBS-free DMEM/F12 in the upper chamber pre-coated with Matrigel, whereas 200 µL of conditioned medium was added into the lower chamber. Next, cells were pre-treated with or without LY294002 or perifosine for 2 h, and then further treated with VAP. After culture at room temperature for 48 h, non-invaded cells on the upper surface were scraped off with a cotton swab, whereas invaded cells were fixed with 4% methanol for 15 min and stained with crystal violet solution (0.1%, C0121, Beyotime) at room temperature for 20 min. Finally, images were photographed from five random fields using a 250× inverted microscope (IX71; Olympus, Tokyo, Japan).

Tube formation assay

In order to determine the effect of VAP on ADSC-induced angiogenesis in human umbilical vein endothelial cells (HUVECs), we carried out the tube formation assay on Matrigel matrix. ADSCs were pre-treated with or without LY294002 or perifosine for 2 h, and then further treated with VAP for 48 h. Next, treated ADSCs were co-cultured with HUVECs for 24 h. Then, these HUVECs (1×10^4 cells/well) were further cultured in 6-well plates pre-coated with Matrigel matrix at 37°C. 6 h of culture later, the tube formation of HUVECs was examined under a 100 × inverted microscope (IX71; Olympus, Tokyo, Japan). Five random microscopic (×100) fields per well were included and relative angiogenesis rate was calculated by tube numbers relative to controls (set as 100%).

Western blot

Proteins were extracted with Cell lysis buffer (P0013, Beyotime) and quantified using a bicinchoninic acid (BCA) protein assay kit (P0013, Beyotime). Then the extracted proteins were isolated by electrophoresis on 10% sodium dodecyl sulfate polyacrylamide gel electrophoresis (SDS-PAGE) gel and transferred onto polyvinylidene fluoride (PVDF) membranes (FFP32, Beyotime). Protein markers (PR1910 (11–180 kDa) and PR1920 (11–245KD)) were purchased from Beijing Solarbio Science & Technology Co., Ltd. Next, the membranes were probed with the primary antibodies (shown in Table 1) at room temperature for 2 h, followed by the incubation with the secondary antibody Goat Anti-Mouse (1:2000, ab205719, Abcam, USA) or Goat Anti-Rabbit (1:2000, ab205718, Abcam, USA) antibody at room temperature for 1 h, and subsequent visualization using BeyoECL Star (P0018FS, Beyotime). Signals were analyzed with a luminescent image analyzer (ImageQuant LAS4000 mini). The expression level of each protein was normalized to the loading controls (β -actin). The raw data were provided in supplemental spreadsheet 1.

Animal model

The construction of chronic skin ulcer model with Yin syndrome in mice referred to literature [3]. We prepared a mouse model of skin ulcer with Yin syndrome using immunosuppression (hydrocortisone) combined with skin wounds and plastic ring (as foreign body). All 50 male KM mice (weight: 20–22 g) purchased from the Vital River Laboratory Animal Technology Co., Ltd. (Beijing, China) were fasted for 12 h with only access to water. After that, femoral muscle of 40 mice was

injected with hydrocortisone injection solution (1,303,011, Tianjin, China, Tianjinkingyork Co., Ltd.) for three days to suppress inflammatory and immune responses. On the 4th day, mice were anesthetized by intraperitoneal injection with 2.5% pentobarbital sodium (40 mg/kg). The anesthetized mice were placed on a fixed plate in the prone position with the limbs fixed, and then the hair on the back was cut off for skin preparation. A circular whole skins and subcutaneous connective tissues with a diameter of about 1.2 cm was surgically removed under sterile conditions. It was carefully operated, away from great vessels and deep into fascia. A sterilized plastic ring (outer diameter 2 cm, inner diameter 1.2 cm, thickness 0.2 cm) was inserted into edge of incision, and was stitched with two single stitches to the skin to prevent shedding. Two weeks later, the secretions on the wound surface were increased significantly, the skin on the wound edge was uneven, and even swelling and induration appeared. The healing trend of wound was not obvious. Moreover, mice ate less, turned emaciated, had shapeless stools, and reduced activities accompanied by curling up, claspings, and cold limbs and tails. The above exhibitions indicated the successful establishment of a skin ulcer model with Yin syndrome. Another 10 mice without a three-day hydrocortisone injection but with skin wounds and plastic ring were assigned into blank group.

Animal groups and treatments

In order to ensure the long-term activity of VAP *in vivo*, PLGA microspheres were used for the sustained release of VAP. VAP-PLGA microspheres were produced by Changchun Institute of Applied Chemistry Chinese Academy of Sciences (Changchun, China). The preparation of VAP-

Table 1. List of primary antibodies used for western blots.

Protein	Antibody	Catalog Number	Company	Antibody Dilution
p-PI3K	Rabbit Anti-p-PI3K antibody	#4228	CST	1:1000
PI3K	Rabbit Anti-PI3K antibody	ab191606	Abcam	1:1000
p-Akt (Ser473)	Rabbit Anti-p-Akt antibody	#9271	CST	1:1000
Akt	Rabbit Anti-Akt antibody	#9272	CST	1:1000
HIF-1 α	Rabbit Anti-HIF-1 α antibody	ab179483	Abcam	1:1000
VEGF	Mouse Anti-VEGFA antibody	ab1316	Abcam	1:100
β -actin	Mouse Anti-beta Actin antibody	ab8226	Abcam	1:1000

PLGA microspheres was as follows: chitosan was dissolved in 3% ice-acetic acid solution and stirred to obtain chitosan-glucic acid solution. VAP-PLGA was dissolved in the chitosan-glucic acid solution to obtain mixed solution. Next, the mixed solution was slowly added to the emulsifier and stirred, and then ultrapure water was added to obtain emulsion. Subsequently, glutaraldehyde was added as a cross-linker to the binding reaction. After being centrifugated and washed by anhydrous ethanol and acetone, the precipitate was dried to obtain VAP-PLGA microspheres.

Following the chronic skin ulcer model establishment for two weeks, 40 mice with Yin syndrome of chronic skin ulcers were assigned to four groups (10 mice/group): model, ADSCs, VAP-PLGA, VAP + ADSCs groups, according to the random digital table method, to determine the role of VAP-PLGA combined with ADSCs in wound healing in chronic skin ulcers. Then, the sterilized plastic ring inserted into the edge of incision was removed from mice. Iodophor (0.5%) was used for wound disinfection and necrotic tissues were removed in each group. Edge and bottom of the wound in the model and blank groups were injected with 100 μ L of PBS. At the same positions as the model and blank groups, mice in the ADSCs group were injected with 100 μ L of PBS containing 1×10^6 ADSCs, those in the VAP-PLGA group were injected with 100 μ L of PBS containing 15 mg/g VAP-PLGA, and those in the VAP-PLGA + ADSCs group were injected with 100 μ L of PBS containing 15 mg/g VAP-PLGA and 1×10^6 ADSCs. Wounds in the above groups were banded by aseptic wound dressing. The mice received treatment one time on the day 0. The changes in wounds and granulation tissue growth were observed with naked eyes on the 0, 14th and 28th days. Also, on the 28th day, more detection was conducted. The dosage and use of the selected VAP and ADSCs were following the reference [39].

Wound healing observation

On the days 0, 14 and 28, the changes in wounds and granulation tissue growth were observed with naked eyes. Meanwhile, all wounds were

photographed with a digital camera (COOLPIX B700, Nikon, Japan). Wound areas were measured with standard transparent square paper. Unhealed wound areas were calculated, and healing curves were drawn. The wound healing rate was calculated using the following equation: wound healing rate = (initial wound areas – unhealed wound areas)/initial wound areas \times 100%.

Hematoxylin and eosin (HE) staining

Histopathological observation of wound tissue structures, as well as distribution of inflammatory cells, fibroblasts and capillary on wound surface in wound healing process was completed by HE staining experiment. On the 28th day, mice were anesthetized by intraperitoneal injection with 2.5% pentobarbital sodium (40 mg/kg), and then wound tissues and surrounding tissues (2 mm in depth and 2 mm in width) were cut off. The collected tissues were immersed and fixed in 10% paraformaldehyde, conventionally embedded into paraffin, cut into sections (5 μ m thick), and stained using a Hematoxylin and Eosin Staining Kit (C0105, Beyotime). Then, histopathological changes in wounds were observed under an inverted microscope at 100 \times and 200 \times magnifications (IX71; Olympus, Tokyo, Japan).

Immunohistochemistry for CD31

CD31 is a marker for blood vessel endothelium. Hence, we used anti-CD31 antibody (1:50, ab28364, Abcam) to examine the capillary vessel in the wound tissues by immunohistochemically staining [19]. Briefly, after routine antigen retrieval, the fixed tissue sections above were incubated with 3% H_2O_2 at room temperature for 10 min, washed with PBS, placed into 0.01 mmol/L citrate buffer (pH 6.0), and then subjected to microwave antigen retrieval for 20 min. Next, the tissue sections were treated with primary CD31 antibody at 4°C overnight, and then probed with the HRP-conjugated goat anti-rabbit polyclonal secondary antibody (1:2000, ab205718, Abcam) at 37°C for 20 min. Since then, the sections were stained with a DAB Horseradish Peroxidase Color Development Kit (P0203, Beyotime) and counterstained with hematoxylin

(C0107, Beyotime), and finally mounted. Yellow or brownish yellow stain indicated that the tissues were CD31-positive. Images were captured using an inverted microscope at 100× and 200× magnifications (IX71; Olympus, Tokyo, Japan).

Quantitative reverse transcription polymerase chain reaction (qRT-PCR)

Total RNA was extracted from wound tissues by the routine Trizol method. Reverse transcription from the RNA was performed using a PrimeScript™ RT reagent Kit (RR036B, Takara). PCR amplification was performed using Thermal Cycler Dice Real-Time System series (Takara) with TB Green® Premix Ex Taq™ II (RR820Q, Takara) based on the manufacturer's instructions. The amplification program was set as follows: pre-denaturation at 95°C for 30 s, followed by 40 cycles of denaturation at 95°C for 5 s and annealing at 60°C for 30 s. The RNA levels were calculated using the $2^{-\Delta\Delta C_t}$ method [40]. Primers used in this experiment were synthesized by Sangon Biotech Co., Ltd. (Shanghai, China) and are depicted in Table 2. The gene level was normalized to β -actin, and expressed relative to the level in the model group (set as 1). The raw data were provided in supplemental spreadsheet 1.

Table 2. Primer sequences used for quantitative reverse transcription polymerase chain reaction (qRT-PCR).

Genes		Primer sequences(5'-3')
VEGF	forward	CTGCCGTCCGATTGAGACC
	reverse	CCCCTCCTTGTAACCACTGTC
SDF-1	forward	TGCATCAGTGACGGTAAACCA
	reverse	TTCTTCAGCCGTGCAACAATC
CXCR4	forward	GAAGTGGGGTCTGGAGACTAT
	reverse	TTGCCGACTATGCCAGTCAAG
Ang-4	forward	CAGCCAGCTATGCTACTAGATGG
	reverse	CAGGCAAGTCCCTCTGGAG
HIF-1 α	forward	CCCCTGTCATCTTTTGCCCT
	reverse	AGCTGGCAGAATAGCTTATTGAG
VEGFR	forward	CTGCCGTCCGATTGAGACC
	reverse	CCCCTCCTTGTAACCACTGTC
TGF- β 1	forward	CCACCTGCAAGACCATCGAC
	reverse	CTGGCGAGCCTTAGITTTGGAC
IL-1 β	forward	GAAATGCCACCTTTTGACAGTG
	reverse	TGGATGCTCTCATCAGGACAG
IL-18	forward	GACTCTTGCCTCAACTCAAGG
	reverse	CAGGCTGTCTTTGTCAACGA
IL-6	forward	TAGTCCTTCTACCCCAATTTC
	reverse	TTGGTCCTTAGCCACTCCTTC
β -actin	forward	ACAGATCTGTGGTGTGGCAC
	reverse	GGCCCCGGATTATCCGACATTC

Statistical analysis

All experiments were performed independently in triplicate. Average data were shown as mean \pm standard deviation and analyzed with SPSS 19.0 software (SPSS, Inc., Chicago, IL, USA). Significant differences between sample groups were analyzed by one-way analysis of variance (ANOVA) followed by Bonferroni's post hoc test where $p < 0.05$ was considered as a significant difference.

Results

This study explored the regulatory role of VAP combined with ADSCs in cutaneous wound healing. We managed to develop combination therapy with ADSCs and VAP-PLGA to improve cutaneous wound healing during chronic skin ulcers. We hypothesized that VAP promoted the proliferation and migration of ADSCs, and PI3K/Akt/HIF-1 α pathway played an important part in the roles of VAP and ADSCs on wound healing. We provided *in vitro* evidence that VAP intensified ADSC proliferation, migration and invasion through the PI3K/Akt/HIF-1 α pathway. In a mouse wound healing model, we claimed that VAP in PLGA microspheres enhanced the promoting effect of ADSC on wound healing. We further investigated the underlying mechanism that PI3K/Akt/HIF-1 α pathway was involved in ADSC-mediated angiogenesis, inflammation inhibition and dermal collagen synthesis.

ADSCs were identified from morphologies and immune phenotypes

As described in Figure 1(a), P1 and P3 ADSCs exhibited adherent growth and spindle- or long fusiform-shaped morphology in an orderly manner, growing in a whirlpool shape, while the cell morphology became more uniform in P3 ADSCs than in P1 ADSCs. The results from flow cytometry assay showed that ADSCs were positive for CD29 (99.44%), CD90 (99.37%), CD73 (99.63%) and CD105 (99.64%), but were negative for CD34 (0.02%) and CD45 (0.03%) (Figure 1(b)). Therefore, the P3 ADSCs were identified as mesenchymal stem cells [41].

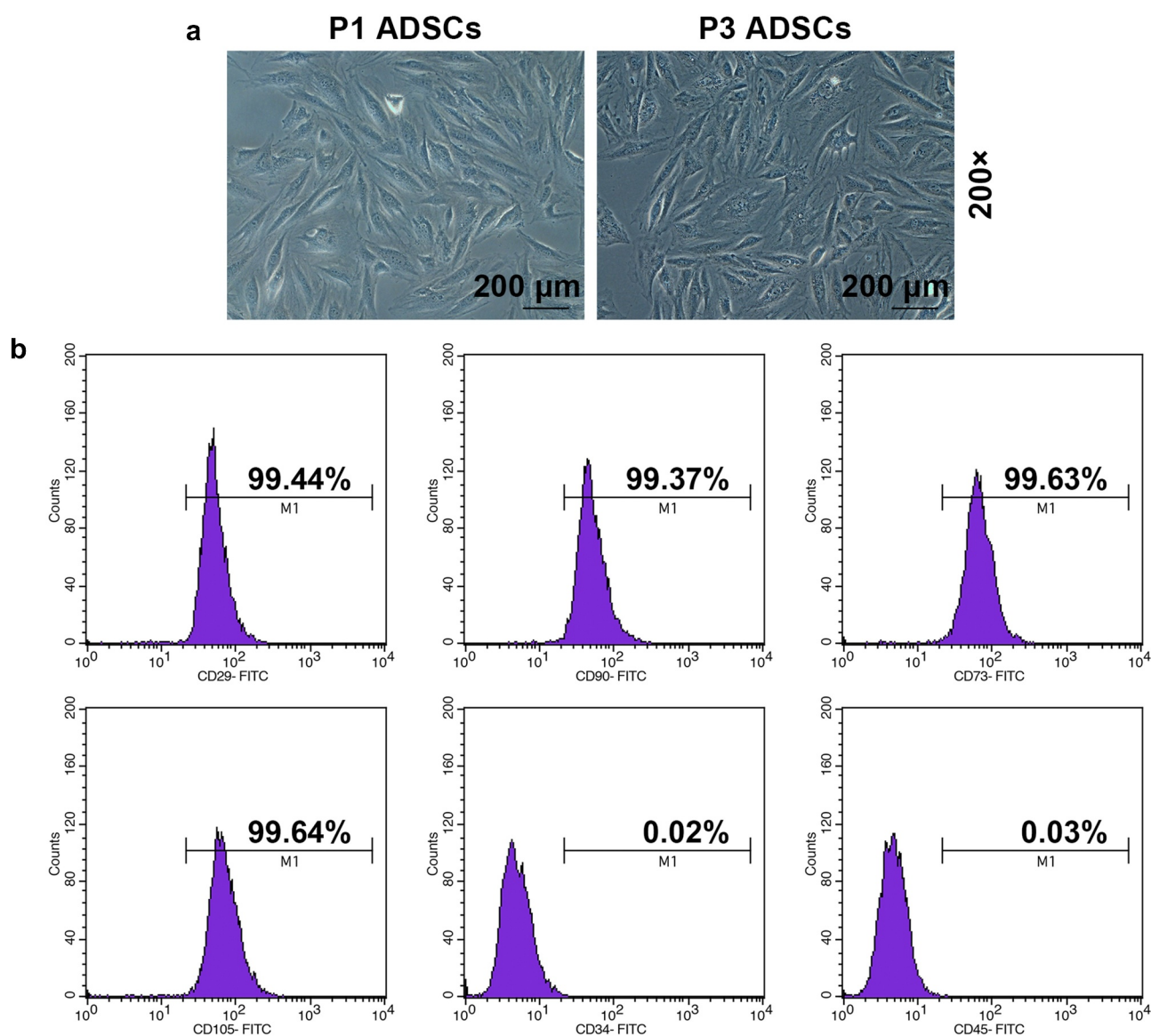


Figure 1. Morphology and immune phenotype of adipose-derived stem cells (ADSCs) were identified by morphological observation and flow cytometry. (a) Morphology of the primary (P1) and third passage (P3) of ADSCs. Images were acquired at 200× magnification. (b) Immune phenotype of ADSCs. The average data from three independent experiments were shown as mean ± standard deviation.

VAP promoted the proliferation, migration, invasion, and angiogenesis of ADSCs

The purity of VAP was determined as 18% by the Kjeldahl method. The viability of ADSCs was remarkably increased in a dose-dependent manner following treatment with VAP at doses of 0, 6, 12, 25, and 50 $\mu\text{g}/\text{mL}$ for 48 h (Figure 2(a), $p < 0.05$). Meantime, the colony formation (Figure 2(b), $p < 0.01$), migration (Figure 2(c), $p < 0.01$), and invasion (Figure 2(d), $p < 0.01$) rates of ADSCs were notably increased after treatment with different doses of VAP, especially 25 $\mu\text{g}/\text{mL}$ VAP. Moreover,

the angiogenesis rate of HUVECs was markedly promoted in a dose-dependent manner following co-culture with VAP-treated ADSCs (VAP at doses of 0, 6, 12, 25, and 50 $\mu\text{g}/\text{mL}$) (Figure 2(e), $p < 0.01$).

VAP promoted the expressions of PI3K/Akt/HIF-1 α signaling pathway-related molecules in ADSCs

VAP at different doses (0, 6, 12, 25 and 50 $\mu\text{g}/\text{mL}$), especially 25 $\mu\text{g}/\text{mL}$, signally promoted the expression of HIF-1 α , and the higher concentration

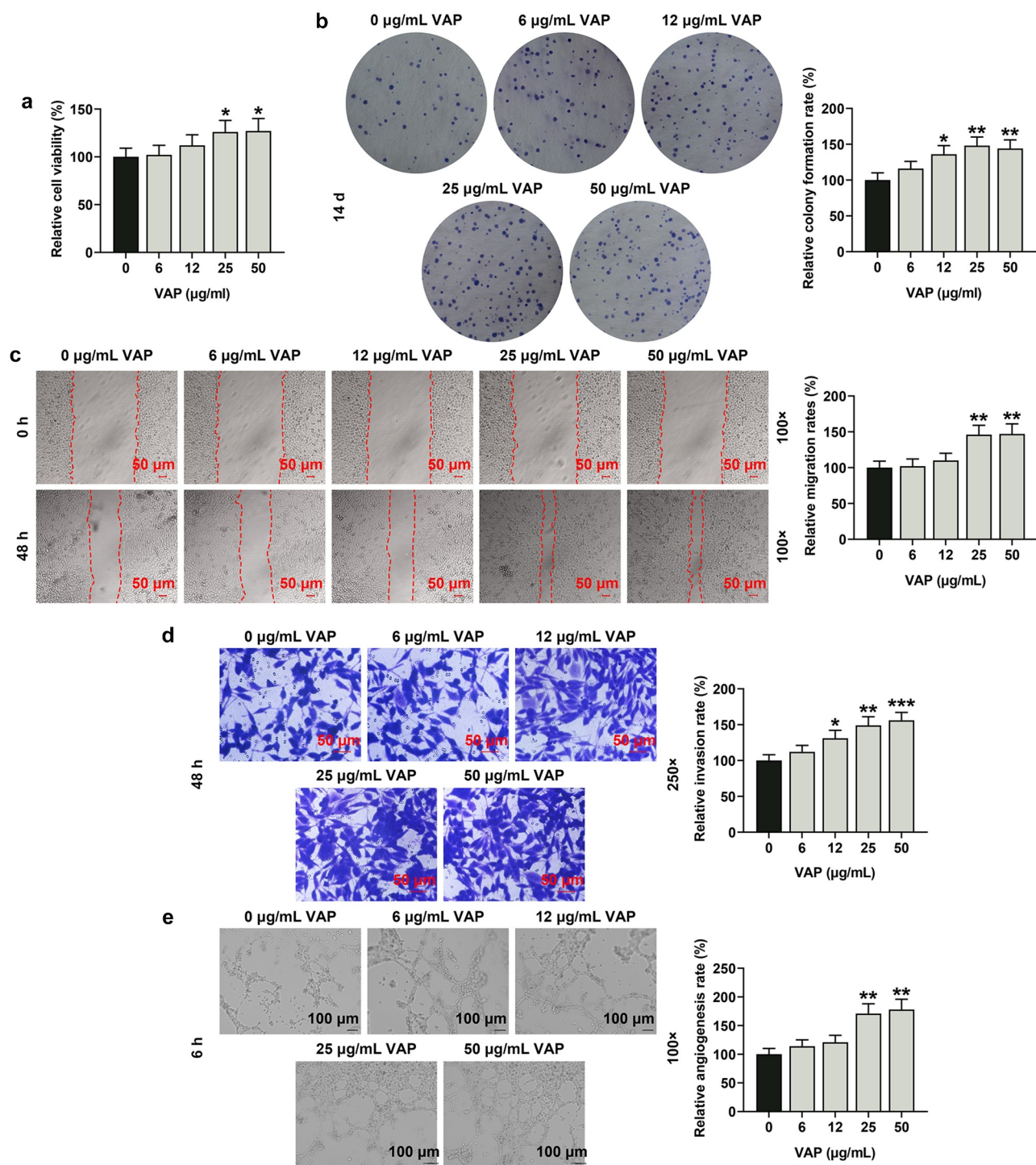


Figure 2. The promoting effect of velvet antler polypeptide (VAP) on the proliferation, migration and invasion rates of adipose-derived stem cells (ADSCs), as well as the angiogenesis rate of HUVECs following co-culture with ADSCs was detected. (a-d) Results from Cell Counting Kit-8 (CCK-8), colony formation, scratch wound healing, and transwell assays showed that VAP treatment generally dose-dependently promoted the viability (a), colony formation (b), migration (c) and invasion (d) rates of ADSCs, respectively. (e) Results from tube formation assay showed that VAP treatment generally dose-dependently promoted the angiogenesis rate of HUVECs following co-culture with ADSCs. Images were acquired at 100× and 250× magnification. The average data from three independent experiments were shown as mean ± standard deviation. * $p < 0.05$ or ** $p < 0.01$ vs. 0 μg/mL VAP.

induced the higher expression of HIF-1α (Figure 3(a, b), $p < 0.01$ or $p < 0.001$). As expected, the levels of p-PI3K/PI3K (Figure 3(a,c), $p < 0.05$), and p-Akt/

Akt (Figure 3(a,d), $p < 0.05$ or $p < 0.01$ or $p < 0.001$) were augmented in a dose-dependent manner after treatment with VAP at varied doses for 48 h.

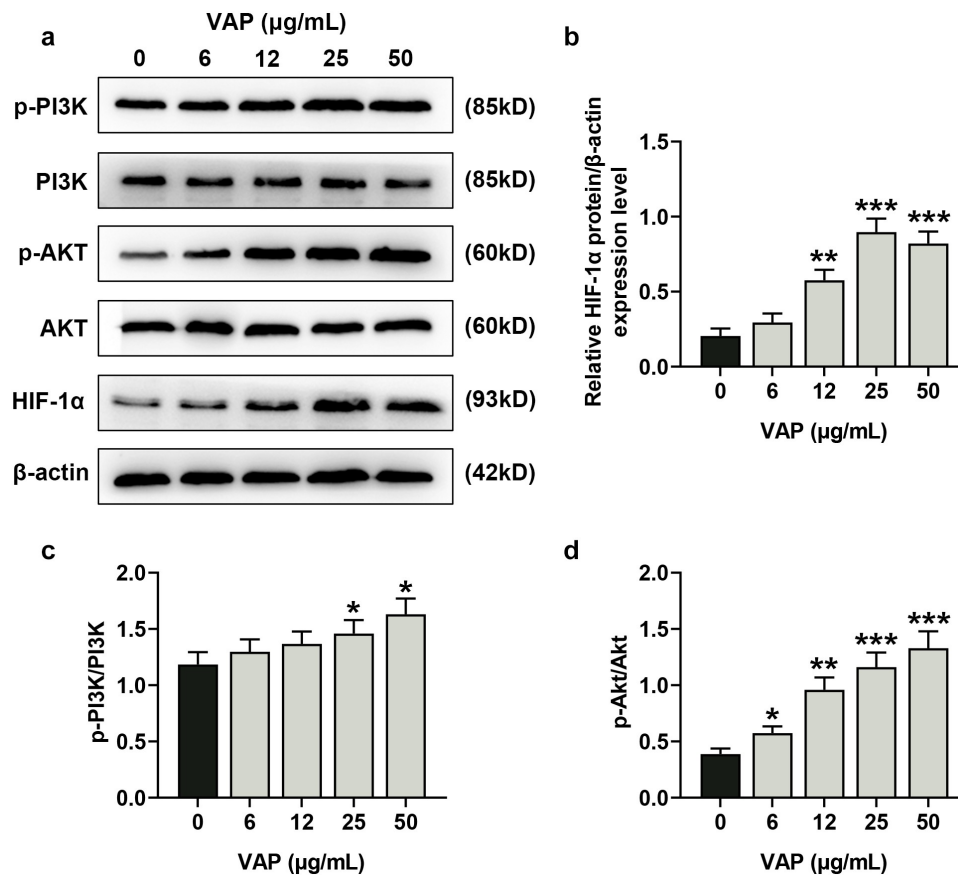


Figure 3. Velvet antler polypeptide (VAP) promoted the expressions of PI3K/Akt/HIF-1 α signaling pathway-related molecules in adipose-derived stem cells (ADSCs). (a) Western blot analysis indicated the protein levels of PI3K, p-PI3K, Akt, p-Akt and HIF-1 α . (b) Relative protein level of HIF-1 α . (c) The ratio of p-PI3K to total PI3K protein (p-PI3K/PI3K). (d) The ratio of p-Akt to total Akt protein (p-Akt/Akt). β -actin was used as an internal control. Images were acquired at 100 \times magnification. The average data from three independent experiments were shown as mean \pm standard deviation. * p < 0.05 or ** p < 0.01 or *** p < 0.001 vs. 0 μ g/mL VAP.

LY294002 and perifosine inhibited the promoting effect of VAP on the proliferation, migration, invasion, and angiogenesis of ADSCs

In view of the above results, 25 μ g/mL VAP was selected and used for the next experiments. First of all, we evaluated the effects of LY294002 and perifosine on VAP-induced promoted proliferation of ADSCs. The results revealed that VAP (25 μ g/mL) treatment overtly boosted the viability (Figure 4(a), p < 0.05) and colony formation (Figure 4(b), p < 0.01) of ADSCs, the tendencies of which were partially reversed by LY294002 (Figure 4(a,b), p < 0.05 or p < 0.01) and perifosine (Figure 4(a,b), p < 0.05 or p < 0.01). Moreover, VAP (25 μ g/mL) treatment evidently advanced the migration (Figure 4(c), p < 0.01) and invasion (Figure 5(a), p < 0.01) of ADSCs, and the angiogenesis rate (Figure 5(b), p < 0.001) of HUVECs was raised following co-culture with 25 μ g/mL

VAP-treated ADSCs, which were partially reversed by LY294002 (Figure 4(c), 5(a,b), p < 0.01 or p < 0.001) and perifosine (Figure 4(c), 5(a,b), p < 0.01 or p < 0.001).

LY294002 and perifosine inhibited the promoting effect of VAP on the expressions of PI3K/Akt/HIF-1 α signaling pathway-related molecules

VAP (25 μ g/mL) treatment observably promoted the phosphorylation of PI3K (Figure 6(a), p < 0.001) and Akt (Figure 6(a), p < 0.01) as well as the expression of HIF-1 α (Figure 6(a), p < 0.01), the tendencies of which were partially overturned by LY294002 (Figure 6(a), p < 0.05 or p < 0.01) and perifosine (Figure 6(a), p < 0.05 or p < 0.01). As expected, the levels of HIF-1 α (Figure 6(a,b), p < 0.05), p-PI3K/PI3K (Figure 6(a-c), p < 0.001), and p-Akt/Akt (Figure 6(a,d), p < 0.01) were up-regulated by VAP

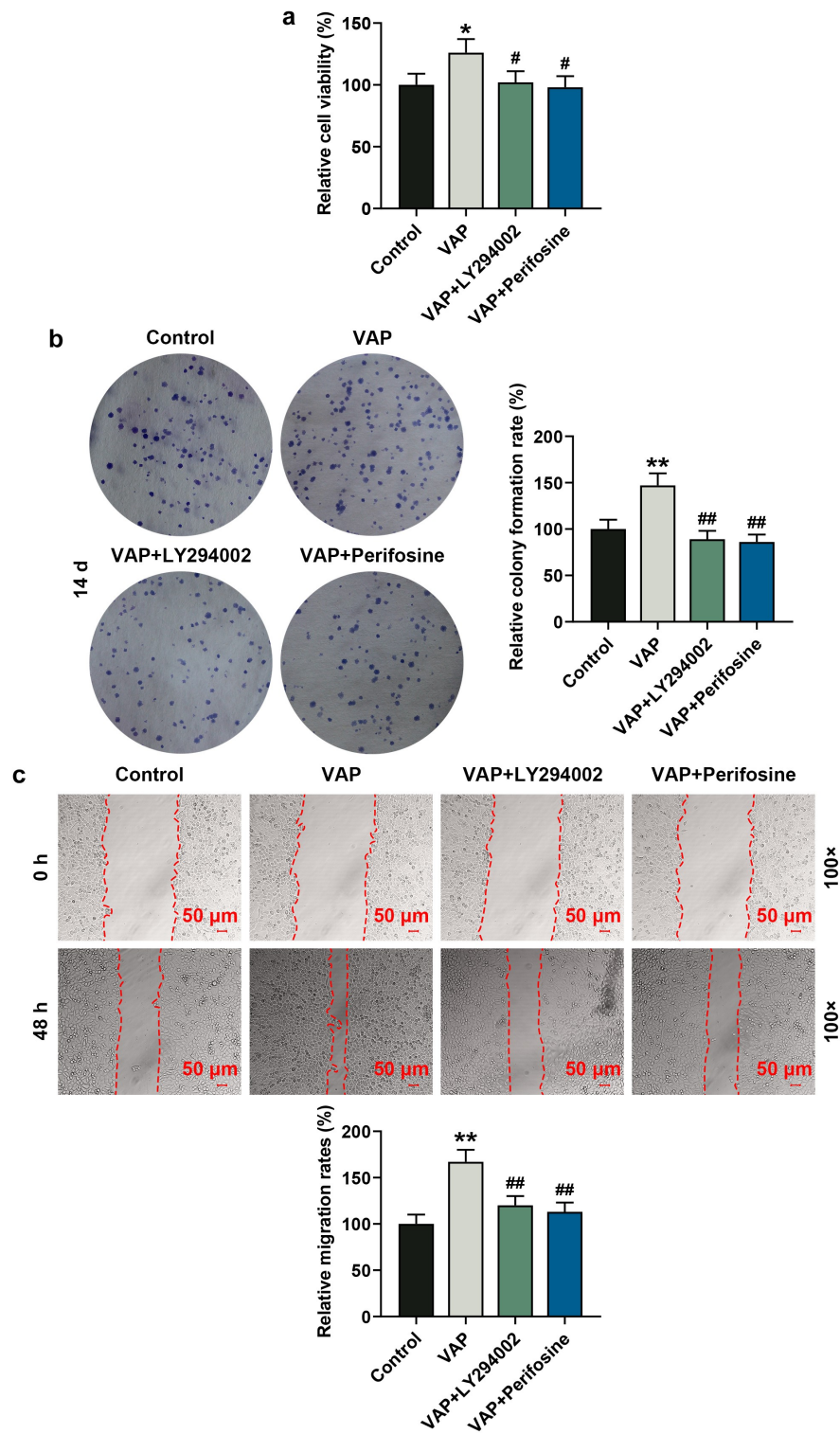


Figure 4. LY294002 and perifosine inhibited the promoting effect of velvet antler polypeptide (VAP) on the proliferation and migration of adipose-derived stem cells (ADSCs). (a-c) The viability (a), colony formation (b), and migration (c) rates of ADSCs in the control, VAP, VAP+LY294002, and VAP+perifosine groups were assessed by CCK-8, colony formation, scratch wound healing and transwell assays, respectively. The average data from three independent experiments were shown as mean \pm standard deviation. * $p < 0.05$ or ** $p < 0.01$ vs. Control; ## $p < 0.01$ vs. VAP.

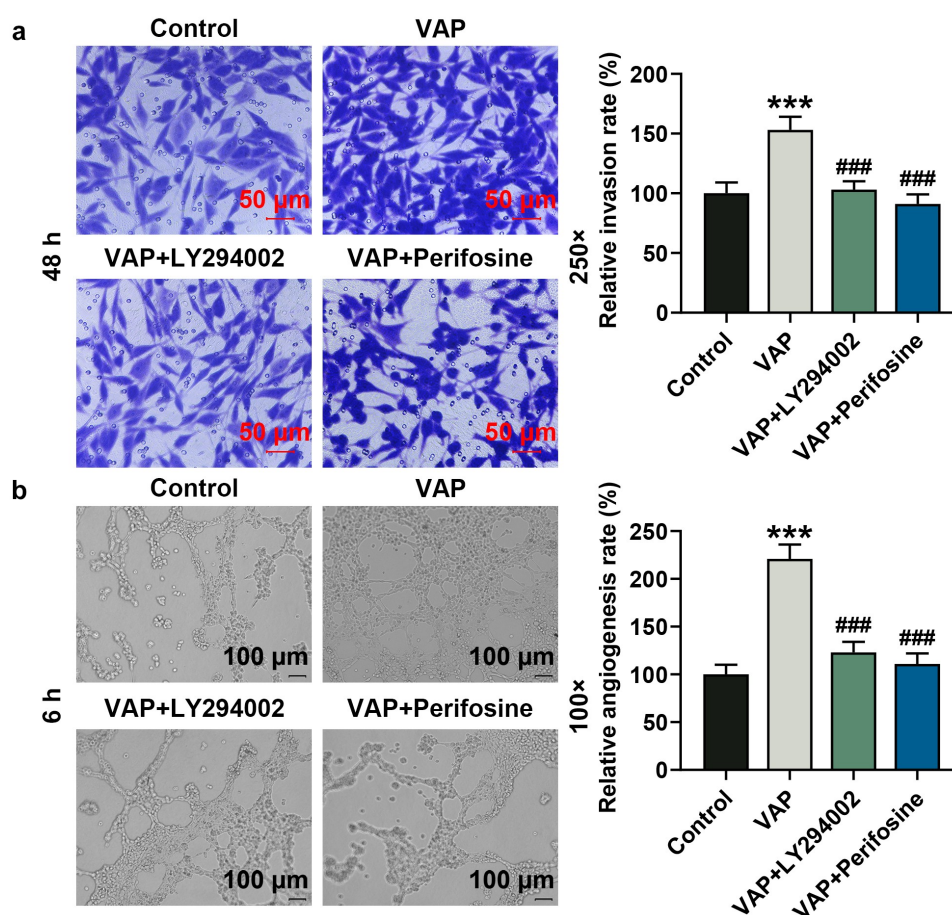


Figure 5. LY294002 and perifosine inhibited the promoting effect of velvet antler polypeptide (VAP) on the invasion of adipose-derived stem cells (ADSCs) and the angiogenesis rate of HUVECs following co-culture with ADSCs. (a) Invasion rates of ADSCs in the control, VAP, VAP+LY294002, and VAP+perifosine groups were determined by invasion assay. (b) Angiogenesis rates of HUVECs following co-culture with ADSCs in the control, VAP, VAP+LY294002, and VAP+perifosine groups were determined by tube formation assay. Images were acquired at 100× and 250× magnifications. The average data from three independent experiments were shown as mean ± standard deviation. ** $p < 0.01$ or *** $p < 0.001$ vs. Control; ## $p < 0.01$ or ### $p < 0.001$ vs. VAP.

(25 $\mu\text{g}/\text{mL}$) treatment, which were partially overturned by LY294002 and perifosine (Figure 6(a-d), $p < 0.001$).

VAP-PLGA enhanced the promoting effect of ADSCs on wound healing in chronic skin ulcers in vivo

As shown in Figure 7(a), on day 0, wounds in all five groups (the blank, model, ADSCs, VAP-PLGA, and VAP-PLGA +ADSCs groups) exhibited full-thickness skin wound deep in fascia, the secretions on the wound surface were increased obviously, the skin on the wound edge was uneven, and even swelling and induration appeared.

By the 14th day, blank group exhibited obvious wound contraction on wound edge, and a small

extent of scab formation appeared on the wound surface; the wound surface in the model group was moist with thin, red, swollen and dim granulation tissues, and exhibited delayed epithelial regeneration; wound surface in the ADSCs group was shrunk and moist; wound surface in the VAP-PLGA group was shrunk and exhibited moist and thin scab cover; and wound surface in the VAP-PLGA +ADSCs group was regular, obviously shrunk and exhibited scab cover. By the 28th day, the wound in blank group was closed and basically healed, with a better recovery; wound in the model group was not closed completely and exhibited scab cover; wound surface in the ADSCs group was shrunk and presented scab cover; and wound surface was shrunk and part of the scab naturally fell off in the VAP-PLGA group. By the

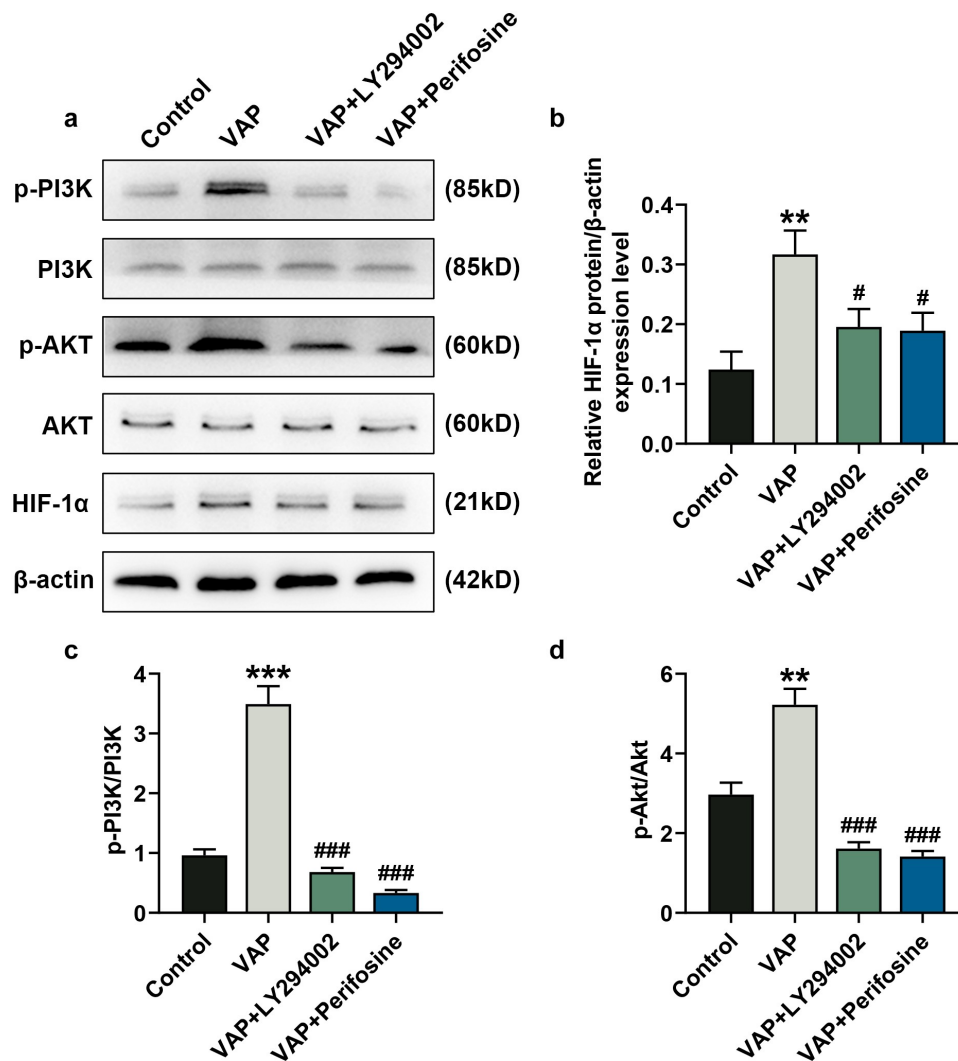


Figure 6. LY294002 and perifosine inhibited the promoting effect of velvet antler polypeptide (VAP) on the expressions of PI3K/Akt/HIF-1 α signaling pathway-related molecules. (a) Western blot analysis indicated the protein levels of PI3K, p-PI3K, Akt, p-Akt and HIF-1 α in the control, VAP, VAP+LY294002, and VAP+perifosine groups. (b) Relative protein level of HIF-1 α . (c) The ratio of p-PI3K to total PI3K protein (p-PI3K/PI3K). (d) The ratio of p-Akt to total Akt protein (p-Akt/Akt). β -actin was used as an internal control. The average data from three independent experiments were shown as mean \pm standard deviation. ** $p < 0.01$ or *** $p < 0.001$ vs. Control; # $p < 0.05$ or ### $p < 0.001$ vs. VAP.

14th and 28th days, compared to the blank group, wound healing rate in the model group was confronted with obvious decline (Figure 7(b), $p < 0.001$). In contrast with the model group, wound healing rate in the ADSCs, VAP-PLGA and VAP-PLGA +ADSCs groups ushered in notable increment (Figure 7(b), $p < 0.01$), with the highest rate in VAP-PLGA +ADSCs group (Figure 7(b), $p < 0.05$).

As mirrored in Figure 8(a), heaps of collagen fibers in the blank group were formed, with thick shape and disordered arrangement; fibroblasts and inflammatory cells as well as obvious collagen

deposition were found in the model group; the ADSCs group appeared a small number of inflammatory cells, loads of fibroblasts, and collagen fibers that were thin, sharp and orderly arranged; collagen fibers in the VAP-PLGA group were well distributed and dense; in the VAP-PLGA +ADSCs group, few inflammatory cells were observed, and collagen fibers were arranged with gap and grew regionally. As can be noticed in Figure 8(b), all the above five groups displayed capillary vessels, reflected by positive CD31 expression. However, CD31 expression in the VAP-PLGA +ADSCs group was more obvious than that in the ADSCs

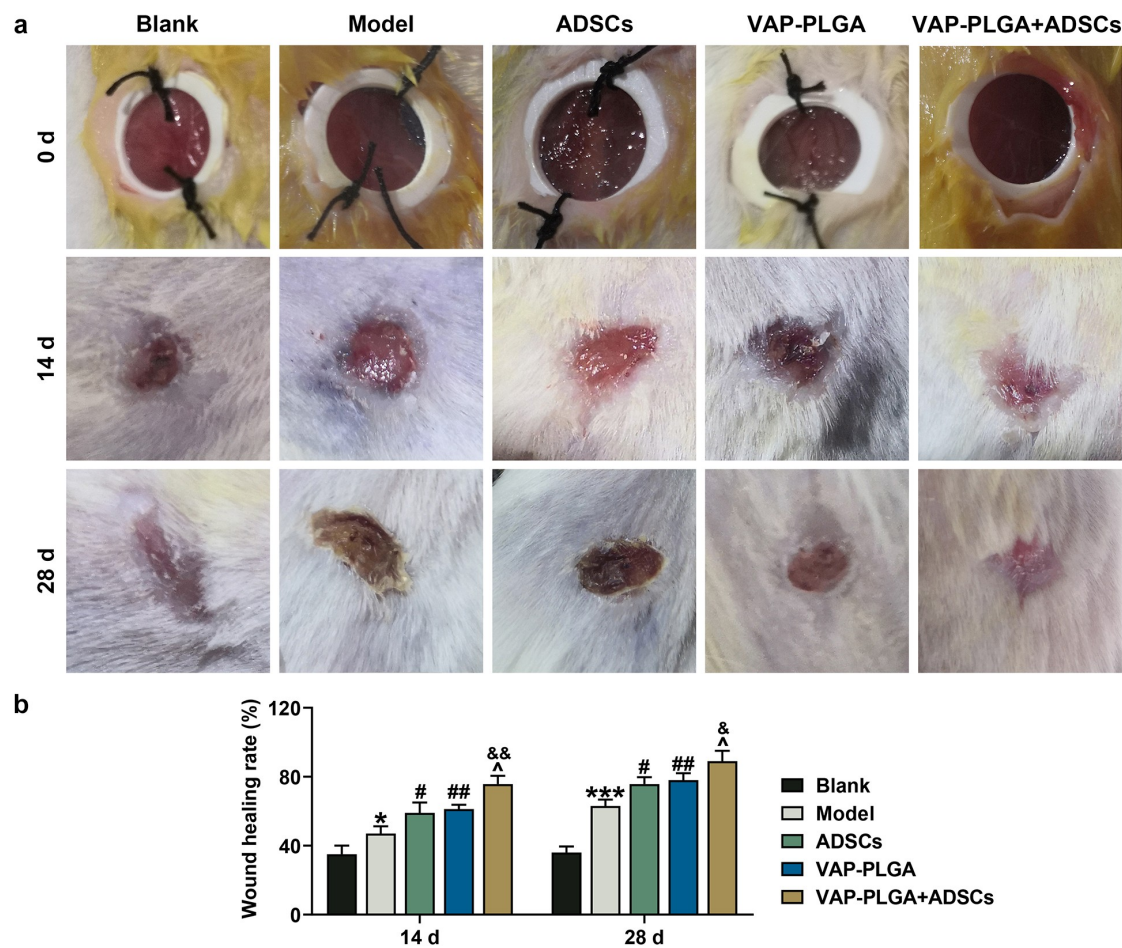


Figure 7. Velvet antler polypeptide (VAP)-PLGA promoted adipose-derived stem cell (ADSC)-induced wound healing in chronic skin ulcers *in vivo*. (a and b) The therapeutic effects of ADSCs or/and VAP (PLGA microspheres) on wound surface in chronic skin ulcers *in vivo* were evaluated by observing pathological changes on the 0, 14th, and 28th days. (a) The wound healing rate on the 28th day (b). The average data from three independent experiments were shown as mean \pm standard deviation. * $p < 0.05$ or *** $p < 0.001$ vs. Blank; # $p < 0.05$ or ## $p < 0.01$ vs. Model; ^ $p < 0.05$ vs. ADSCs; & $p < 0.05$ vs. VAP-PLGA.

and VAP-PLGA groups; and CD31 expression in the VAP-PLGA and ADSCs groups was more notable than that in the model group.

VAP-PLGA enhanced the activating effect of ADSCs on PI3K/Akt/HIF-1 α signaling pathway in chronic skin ulcers *in vivo*

The levels of HIF-1 α , VEGF, p-PI3K/PI3K and p-Akt/Akt were increased in the model group when compared with those in the blank group (Figure 9(a-e), $p < 0.05$). By contrast, these levels were further promoted in the ADSCs and VAP-PLGA groups (Figure 9(a-e), $p < 0.05$ or $p < 0.01$ or $p < 0.001$). Moreover, these levels were higher in ADSCs + VAP-PLGA group than those in ADSCs and VAP-PLGA groups (Figure 9(a-e),

$p < 0.05$ or $p < 0.01$ or $p < 0.001$). In addition, the mRNA level of HIF-1 α was increased in the ADSCs and VAP-PLGA groups (Figure 10(e), $p < 0.001$), which was still lower than that in the VAP-PLGA +ADSCs group (Figure 10(e), $p < 0.01$).

VAP-PLGA enhanced the regulatory effect of ADSCs on the expressions of wound healing-related molecules

Initially, we found that the mRNA level of VEGF was up-regulated in the model group compared with that in the blank group (Figure 10(a), $p < 0.05$); such mRNA level was up-regulated in the VAP-PLGA and ADSCs groups as compared to that in the model group (Figure 10(a), $p < 0.01$);

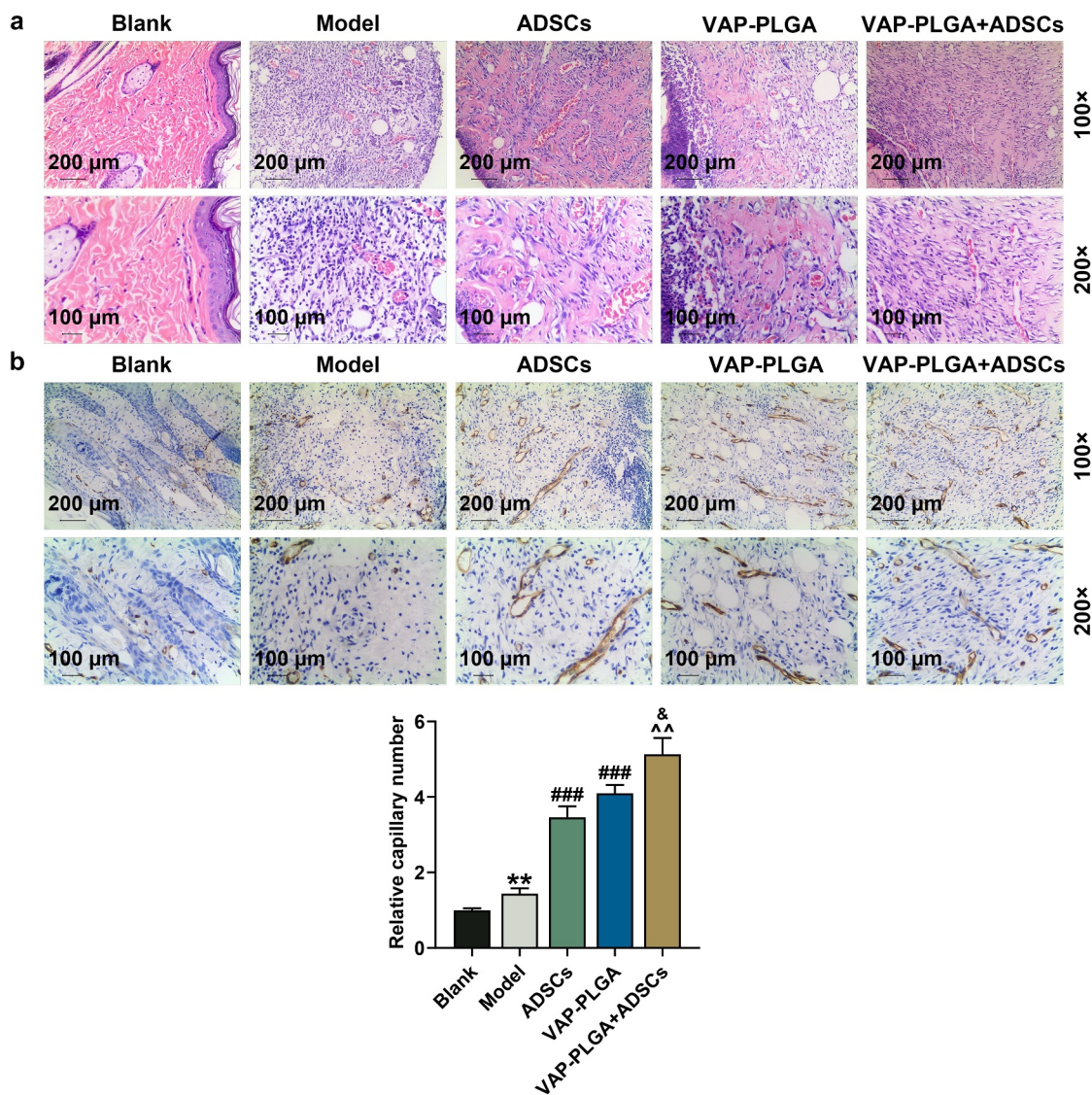


Figure 8. Velvet antler polypeptide (VAP)-PLGA promoted adipose-derived stem cell (ADSC)-induced wound healing in chronic skin ulcers *in vivo*. (a and b) Pathological changes (a) and capillary vessels (b) of wound tissue sections in the blank, model, ADSCs, VAP-PLGA, and VAP-PLGA +ADSCs groups were observed by HE staining and immunohistochemistry for CD31 respectively on the 28th day after treatment. Images were acquired at 100 \times and 200 \times magnifications. The average data from three independent experiments were shown as mean \pm standard deviation. ** $p < 0.01$ vs. Blank; ### $p < 0.001$ vs. Model; ^^ $p < 0.01$ vs. ADSCs; & $p < 0.05$ vs. VAP-PLGA.

and such mRNA level was also up-regulated in the VAP-PLGA +ADSCs group when compared with that in the VAP-PLGA and ADSCs groups (Figure 10(a), $p < 0.05$ or $p < 0.01$). Moreover, we discovered that the mRNA levels of VEGF receptor (VEGFR), stromal cell-derived factor-1 (SDF-1), CXCR4 and Ang-4 were promoted in the ADSCs and VAP-PLGA groups compared with those in model group (Figure 10(b-f), $p < 0.05$ or $p < 0.01$); by contrast, such mRNA levels were further increased in the VAP-PLGA +ADSCs groups (Figure 10(b-f), $p < 0.05$ or

$p < 0.01$). In addition, the mRNA level of TGF- β 1 was increased in the ADSCs and VAP-PLGA groups (Figure 10(g), $p < 0.01$), and in comparison, the mRNA level of TGF- β 1 was further up-regulated in VAP-PLGA +ADSCs groups (Figure 10(g), $p < 0.01$). Besides, the mRNA levels of interleukin-1 β (IL-1 β), IL-18 and IL-6 were dwindled in the ADSCs and VAP-PLGA groups (Figure 10(h-j), $p < 0.05$ or $p < 0.01$), which were still higher than those in the VAP-PLGA +ADSCs groups (Figure 10(h-j), $p < 0.05$ or $p < 0.01$).

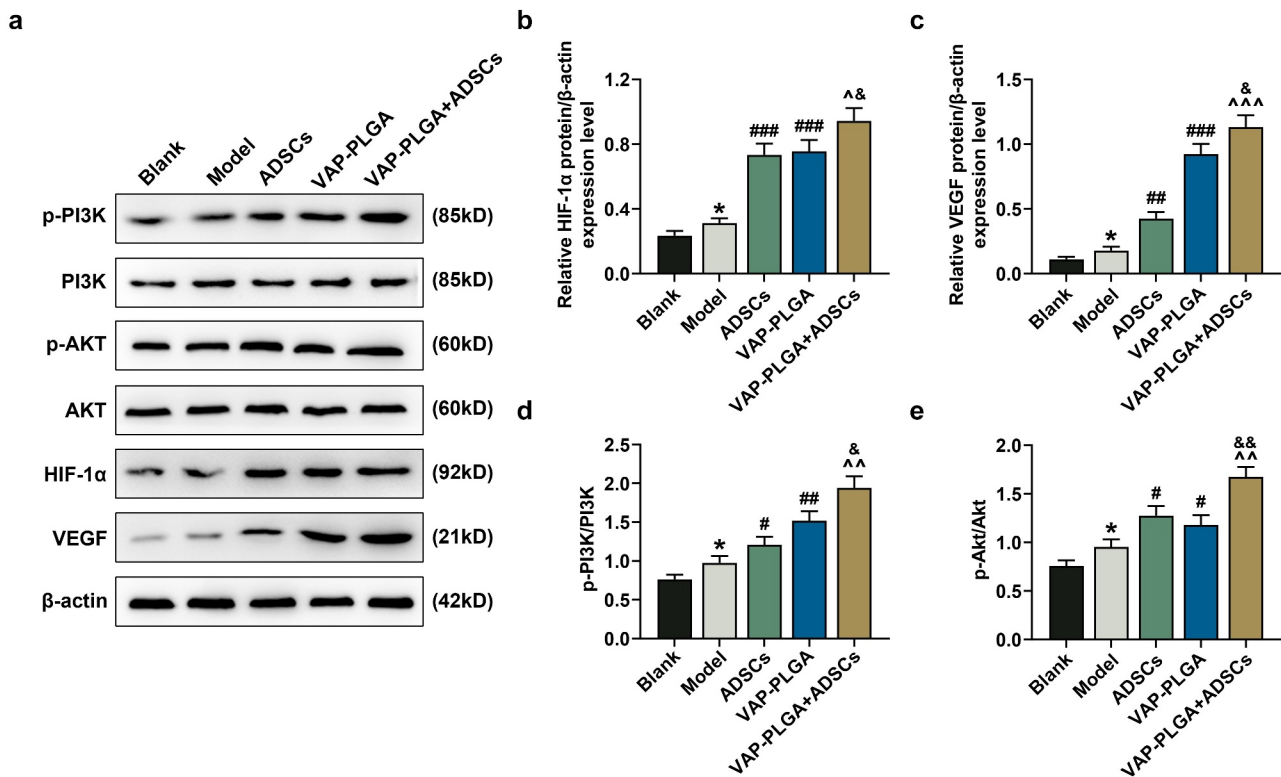


Figure 9. VAP-PLGA enhanced the promoting effect of adipose-derived stem cells (ADSCs) on the activation of PI3K/Akt/HIF-1 α signaling pathway and VEGF expression in chronic skin ulcers *in vivo*. (a) Western blot analysis indicated the protein levels of p-PI3K, PI3K, p-Akt, Akt, HIF-1 α , and VEGF in the blank, model, ADSCs, VAP-PLGA, and VAP-PLGA +ADSCs groups on the 28th day after treatment. (b) Relative protein level of HIF-1 α . (c) Relative protein level of VEGF. (d) The ratio of p-PI3K to total PI3K protein (p-PI3K/PI3K) in the blank, model, ADSCs, VAP-PLGA, and VAP-PLGA +ADSCs groups. (e) The ratio of p-Akt to total Akt protein (p-Akt/Akt) in the blank, model, ADSCs, VAP-PLGA, and VAP-PLGA +ADSCs groups. β -actin was used as an internal control. The average data from three independent experiments were shown as mean \pm standard deviation. * $p < 0.05$ vs. Blank; # $p < 0.05$ or ## $p < 0.01$ or ### $p < 0.001$ vs. Model; ^ $p < 0.05$ or ^^ $p < 0.01$ or ^^ $p < 0.001$ vs. ADSCs; & $p < 0.05$ or && $p < 0.01$ vs. VAP-PLGA.

Discussion

Chronic skin ulcers are rather hard to heal spontaneously. ADSCs have been identified as a particularly promising therapeutic strategy for these wounds by virtue of their well-confirmed efficacies [42], which could promote wound healing by intradermal injection or using the tissue engineering technique [43,44].

Stem cell therapy is costly and the cell survival rate is extremely low. Polypeptides consist of amino acids, and VAP rich in amino acids [45]. VAP could promote cell proliferation [8], exhibit immunomodulatory effects [46], and suppress inflammation [12]. In the present study, we demonstrated that VAP treatment generally dose-dependently promoted the viability, proliferation, colony formation, migration and invasion rates of ADSCs and the angiogenesis rate of HUVECs co-cultured with ADSCs, which would be

partially abrogated when PI3K/Akt/HIF-1 α pathway was blocked. Thus, we could speculate that the angiogenesis of HUVECs could be boosted through the activated PI3K/Akt pathway [47].

We therefore further probed into whether VAP treatment can promote the beneficial effect of ADSCs on wound healing. The main problems with the application of VAP are its short half-life and susceptibility to the degradation of various proteases within the organism. VAP with PLGA microspheres, as a long-acting slow-release dosage form, effectively improves its bioavailability. In the present study, VAP with PLGA microspheres enhanced the promoting effect of ADSCs on wound surface repair, pathological changes and the angiogenesis rate of chronic skin ulcers *in vivo*. A similar report validated that topical treatment with an elk velvet antler water-soluble extract promoted the healing of

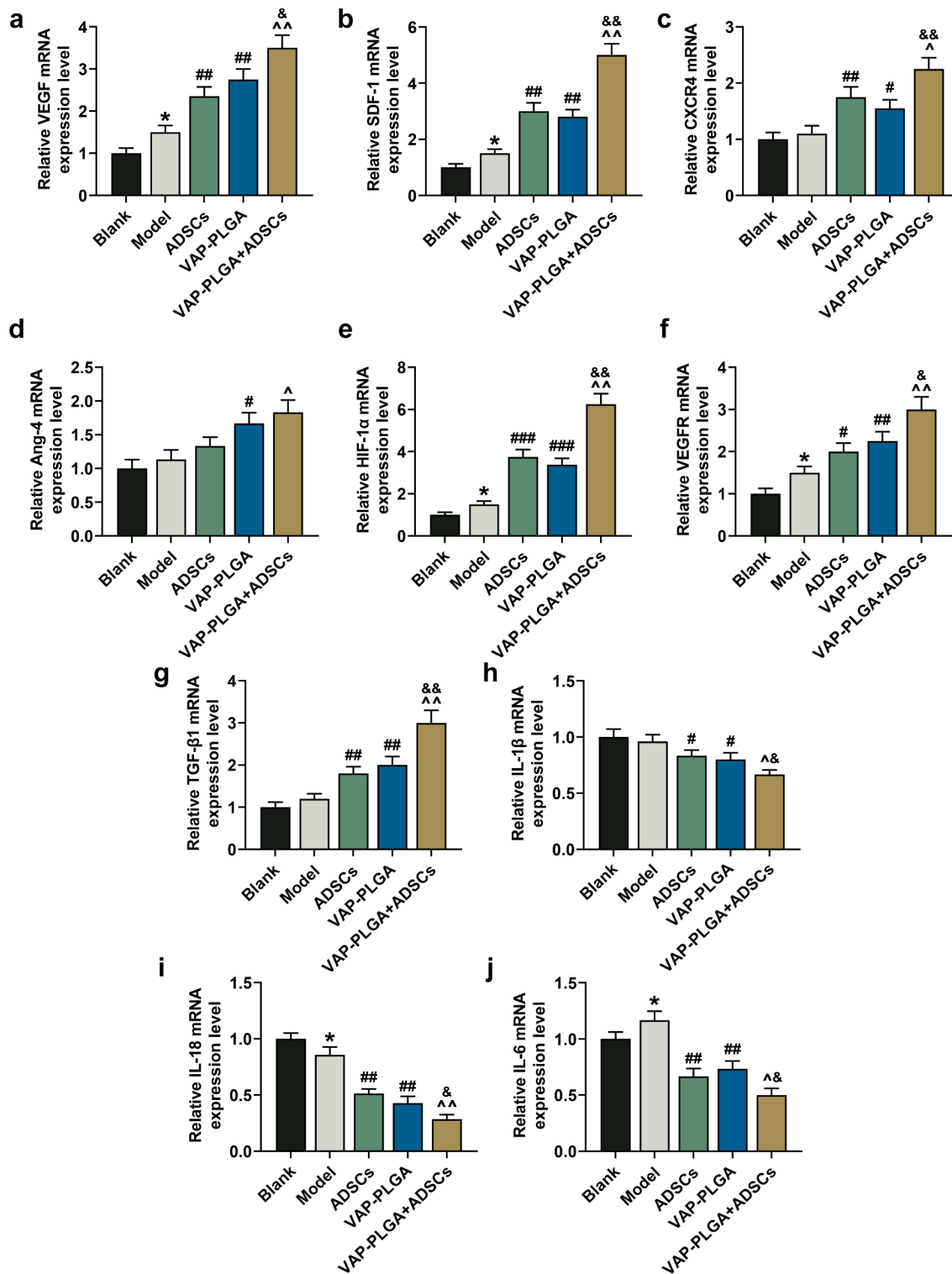


Figure 10. Velvet antler polypeptide (VAP)-PLGA enhanced the regulatory effect of adipose-derived stem cells (ADSCs) on the expressions of wound healing-related molecules and HIF-1 α in chronic skin ulcers *in vivo*. QRT-PCR indicated the mRNA levels of VEGF (a), SDF-1 (b), CXCR4 (c), Ang-4 (d), HIF-1 α (e), VEGFR (f), TGF- β 1 (g), IL-1 β (h), IL-18 (i), and IL-6 (j) in the blank, model, ADSCs, VAP-PLGA, and VAP-PLGA +ADSCs groups on the 28th day after treatment. β -actin was used as an internal control. The average data from three independent experiments were shown as mean \pm standard deviation. *p < 0.05 vs. Blank; #p < 0.05 or ##p < 0.01 or ###p < 0.001 vs. Model; ^p < 0.05 or ^^p < 0.01 vs. ADSCs; &p < 0.05 or &&p < 0.01 vs. VAP. qRT-PCR: quantitative reverse transcriptase PCR; VEGF: vascular endothelial growth factor; SDF-1: stromal cell-derived factor-1; CXCR4: C-X-C motif chemokine receptor 4; Ang-4: angiopoietin-4; VEGFR: VEGF receptor; TGF- β 1: transforming growth factor- β 1; IL: interleukin.

cutaneous wounds in diabetic rats [6]. In addition to the effect of activating PI3K/Akt/HIF-1 α pathway, VAP treatment was also found to enhance the promoting effect of ADSCs on the expressions of angiogenesis-related VEGF, VEGFR, and Ang-4 in wound tissues in chronic skin ulcers *in vivo* as well as on the expressions of TGF- β 1 and chemokine SDF-1 and its receptor CXCR4, and also strengthened the inhibitory effect of ADSCs on the expressions of inflammatory factors IL-1 β , IL-18, and IL-6.

Wound healing is a well-orchestrated cascade process that depends on intricate interactions between different cell types, signaling factors and connective tissue substances. Wound repair is related to inflammation, migration, proliferation and other cellular activities, involving various growth factors and cytokines [48]. During wound healing, ADSCs are known to proliferate and differentiate into skin cells to repair damaged or dead cells, may induce cell repair and activate the healing process via an autocrine and paracrine pathway [49], and are recruited rapidly into the wound site through the great migration ability [44]. Angiogenesis may occur during wound healing and occupy a pivotal position in the process [50,51]. Up-regulated expressions of growth factors VEGF, VEGFR, and Ang-4 play important roles in granulation tissue matrix formation, wound re-epithelialization and scar tissue formation by facilitating vascular regeneration, local blood supply, the division, proliferation and differentiation of fibroblasts and epithelial cells, extracellular matrix synthesis and collagen production [52]. TGF- β 1 accelerates wound healing through multiple pathways that affect cell infiltration, proliferation and angiogenesis, extracellular matrix synthesis and remodeling [53]. A previous report confirmed that ADSC treatment up-regulates the levels of TGF- β 1 and VEGF in wound environments [31]. VEGF is considered as a critical regulator of angiogenesis [54], while TGF- β 1 plays a role in matrix deposition, cellular migration and wound contraction [55]. What is more, Guo et al. reported that SDF-1/CXCR4 is a major regulator involved in the migration of epidermal stem cells during wound repair [56]. Immediate inflammatory response, which is defined as an infiltration of cytokine-releasing leukocytes, occurs in the process of wound healing [57]. Our results demonstrated that VAP meliorates

ADSC-induced wound healing in chronic skin ulcers by promoting angiogenic growth factors and dermal collagen synthesis, enhancing cell migration, and inhibiting inflammatory response, which might involve the activation of PI3K/Akt/HIF-1 α pathway. Besides, VAP-PLGA can reinforce the effect of ADSCs in all stages of wound healing, thereby providing a novel method for wound repair; however, its efficacy and safety in wound treatment still need to be confirmed in more research. Meanwhile, further exploration and research on VAP are also required. It is hoped that we can apply the combined treatment of VAP with ADSCs to promote wound healing in clinic, and provide a safe, effective, economical and convenient treatment for patients suffering from chronic skin ulcers in the future.

Nevertheless, neither an *in vivo* study using co-injection with LY294002/perifosine and VAP/ADSC, nor more intervention methods or therapies were employed in our study, which might be limitations to the current study.

Conclusion

VAP can promote the proliferation, migration, and invasion of ADSCs by activating PI3K/Akt/HIF-1 α pathway, and VAP-PLGA reinforces the function of ADSCs in promoting wound healing in chronic skin ulcers by promoting angiogenic growth factors and dermal collagen synthesis, enhancing cell migration, and inhibiting inflammatory response.

Disclosure statement

No potential conflict of interest was reported by the authors.

Funding

The authors reported there is no funding associated with the work featured in this article.

Availability of Data and Materials

The analyzed data sets generated during the study are available from the corresponding author on reasonable request.

Authors' contributions

Substantial contributions to conception and design: Wen Jiang, Jun Zhang.

Data acquisition, data analysis and interpretation: Xudong Zhang, Chenghong Fan, Jinlong Huang.

Drafting the article or critically revising it for important intellectual content: Wen Jiang, Jun Zhang.

Final approval of the version to be published: Wen Jiang, Jun Zhang, Xudong Zhang, Chenghong Fan, Jinlong Huang.

Agreement to be accountable for all aspects of the work in ensuring that questions related to the accuracy or integrity of the work are appropriately investigated and resolved: Wen Jiang, Jun Zhang, Xudong Zhang, Chenghong Fan, Jinlong Huang.

ORCID

Jinlong Huang  <http://orcid.org/0000-0003-3504-7477>

References

- [1] Denstedt M, Pukstad B, Paluchowski L, et al. Hyperspectral imaging as a diagnostic tool for chronic skin ulcers. *SPIE*. 2013;8565:85650N.
- [2] Liu Y, Shi JP, Xiong W, et al. Production of an animal model of semi-yin and semi-yang syndrome with diabetic ulcers and study of its pathological and metabolic features. *Evid Based Complement Alternat Med*. 2021;2021:6345147.
- [3] Chai Z, Lv Y. Exploration and discussion of the establishment of yin syndrome skin ulcer model in Kunming species mice. *J Liaoning Univ Tradit Chin Med*. 2016;18:55–58.
- [4] Kirby GT, Mills SJ, Cowin AJ, et al. Stem cells for cutaneous wound healing. *Biomed Res Int*. 2015;2015:285869.
- [5] Sharma GD, He J, Bazan HE. p38 and ERK1/2 coordinate cellular migration and proliferation in epithelial wound healing: evidence of cross-talk activation between MAP kinase cascades. *J Biol Chem*. 2003;278(24):21989–21997.
- [6] Mikler JR, Theoret CL, High JC. Effects of topical elk velvet antler on cutaneous wound healing in streptozotocin-induced diabetic rats. *J Altern Complement Med*. 2004;10(5):835–840.
- [7] Sui Z, Zhang L, Huo Y, et al. Bioactive components of velvet antlers and their pharmacological properties. *J Pharm Biomed Anal*. 2014;87:229–240.
- [8] Zha E, Gao S, Pi Y, et al. Wound healing by a 3.2 kDa recombinant polypeptide from velvet antler of *Cervus nippon temminck*. *Biotechnol Lett*. 2012;34:789–793.
- [9] He X, Lin Y, Zhao J, et al. Research progress on application of huiyang shengji ointment in chronic skin ulcer. *Chinese Archives of TCM*. 2018;36:2071–2073.
- [10] Zhao L, Mi Y, Guan H, et al. Velvet antler peptide prevents pressure overload-induced cardiac fibrosis via transforming growth factor (TGF)-beta1 pathway inhibition. *Eur J Pharmacol*. 2016;783:33–46.
- [11] Zhu W, Wang H, Zhang W, et al. Protective effects and plausible mechanisms of antler-velvet polypeptide against hydrogen peroxide induced injury in human umbilical vein endothelial cells. *Can J Physiol Pharmacol*. 2017;95(5):610–619.
- [12] Zhao L, Wang X, Zhang XL, et al. Purification and identification of anti-inflammatory peptides derived from simulated gastrointestinal digests of velvet antler protein (*Cervus elaphus Linnaeus*). *J Food Drug Anal*. 2016;24(2):376–384.
- [13] Jia XY, Lai-Jin LU. Experimental study of VAP-chitosans-honey suspension on the healing of decubitus ulcer in swines. *OJC*. 2010;18(6):498–502.
- [14] Guan SW, Duan LX, Li YY, et al. A novel polypeptide from *Cervus nippon temminck* proliferation of epidermal cells and NIH3T3 cell line. *Acta Biochim Pol*. 2006;53(2):395–397.
- [15] Ni H, Zhao Y, Ji Y, et al. Adipose-derived stem cells contribute to cardiovascular remodeling. *Aging (Albany NY)*. 2019;11(23):11756–11769.
- [16] Dominici M, Le Blanc K, Mueller I, et al. Minimal criteria for defining multipotent mesenchymal stromal cells the international society for cellular therapy position statement. *Cytotherapy*. 2006;8(4):315–317.
- [17] Lv FJ, Tuan RS, Cheung KM, et al. Concise review: the surface markers and identity of human mesenchymal stem cells. *Stem Cells*. 2014;32(6):1408–1419.
- [18] Lee EY, Xia Y, Kim WS, et al. Hypoxia-enhanced wound-healing function of adipose-derived stem cells: increase in stem cell proliferation and up-regulation of VEGF and bFGF. *Wound Repair Regen*. 2009;17(4):540–547.
- [19] Han D, Huang W, Ma S, et al. Ghrelin improves functional survival of engrafted adipose-derived mesenchymal stem cells in ischemic heart through PI3K/Akt signaling pathway. *Biomed Res Int*. 2015;2015:858349.
- [20] Bader AG, Kang S, Zhao L, et al. Oncogenic PI3K deregulates transcription and translation. *Nat Rev Cancer*. 2005;5(12):921–929.
- [21] Cain RJ, Vanhaesebroeck B, Ridley AJ. The PI3K p110alpha isoform regulates endothelial adherens junctions via Pyk2 and Rac1. *J Cell Biol*. 2010;188(6):863–876.
- [22] Hou B, Cai W, Chen T, et al. Vaccarin hastens wound healing by promoting angiogenesis via activation of MAPK/ERK and PI3K/AKT signaling pathways in vivo. *Acta Cir Bras*. 2020;34(12):e201901202.
- [23] Han N, Jia L, Su Y, et al. *Lactobacillus reuteri* extracts promoted wound healing via PI3K/AKT/ β -catenin/TGF β 1 pathway. *Stem Cell Res Ther*. 2019;10(1):243.
- [24] Yu T, Gao M, Yang P, et al. Insulin promotes macrophage phenotype transition through PI3K/Akt and

- PPAR- γ signaling during diabetic wound healing. *J Cell Physiol.* **2019**;234(4):4217–4231.
- [25] Li JY, Ren KK, Zhang WJ, et al. Human amniotic mesenchymal stem cells and their paracrine factors promote wound healing by inhibiting heat stress-induced skin cell apoptosis and enhancing their proliferation through activating PI3K/AKT signaling pathway. *Stem Cell Res Ther.* **2019**;10(1):247.
- [26] Xiao W, Tang H, Wu M, et al. Ozone oil promotes wound healing by increasing the migration of fibroblasts via PI3K/Akt/mTOR signaling pathway. *Biosci Rep.* **2017**;37(6):BSR20170658.
- [27] Wang Q, Zhang N, Hu L, et al. Integrin beta1 in adipose-derived stem cells accelerates wound healing via activating PI3K/AKT pathway. *Tissue Eng Regen Med.* **2020**;17(2):183–192.
- [28] Zhang W, Bai X, Zhao B, et al. Cell-free therapy based on adipose tissue stem cell-derived exosomes promotes wound healing via the PI3K/Akt signaling pathway. *Exp Cell Res.* **2018**;370(2):11756–11769.
- [29] Xiao X, Xu S, Li L, et al. The effect of velvet antler proteins on cardiac microvascular endothelial cells challenged with ischemia-Hypoxia. *Front Pharmacol.* **2017**;8:601.
- [30] Yu SP, Wei Z, Wei L. Preconditioning strategy in stem cell transplantation therapy. *Transl Stroke Res.* **2013**;4(1):76–88.
- [31] Fukuda R, Kelly B, Semenza GL. Vascular endothelial growth factor gene expression in colon cancer cells exposed to prostaglandin E2 is mediated by hypoxia-inducible factor 1. *Cancer Res.* **2003**;63:2330–2334.
- [32] Bosch-Marce M, Okuyama H, Wesley JB, et al. Effects of aging and hypoxia-inducible factor-1 activity on angiogenic cell mobilization and recovery of perfusion after limb ischemia. *Circ Res.* **2007**;101(12):1310–1318.
- [33] Chen C, Tang Q, Zhang Y, et al. Metabolic reprogramming by HIF-1 activation enhances survivability of human adipose-derived stem cells in ischaemic microenvironments. *Cell Prolif.* **2017**;50(5):e12363.
- [34] Esfahani M, Karimi F, Afshar S, et al. Prolyl hydroxylase inhibitors act as agents to enhance the efficiency of cell therapy. *Expert Opin Biol Ther.* **2015**;15(12):1739–1755.
- [35] Ortiz-Barahona A, Villar D, Pescador N, et al. Genome-wide identification of hypoxia-inducible factor binding sites and target genes by a probabilistic model integrating transcription-profiling data and in silico binding site prediction. *Nucleic Acids Res.* **2010**;38(7):2332–2345.
- [36] Yamakawa M, Liu LX, Belanger AJ, et al. Expression of angiopoietins in renal epithelial and clear cell carcinoma cells: regulation by hypoxia and participation in angiogenesis. *Am J Physiol Renal Physiol.* **2004**;287(4):F649–57.
- [37] Yamakawa M, Liu LX, Date T, et al. Hypoxia-inducible factor-1 mediates activation of cultured vascular endothelial cells by inducing multiple angiogenic factors. *Circ Res.* **2003**;93(7):664–673.
- [38] Wahl EA, Fierro FA, Peavy TR, et al. In vitro evaluation of scaffolds for the delivery of mesenchymal stem cells to wounds. *Biomed Res Int.* **2015**;2015:108571.
- [39] Gong Q, Song Q, Qiu L, et al. Effects and mechanism of VAP-loaded PLGA microspheres combined with BMSCs on sciatic nerve injury repair in rats. *Traditional Chinese Drug Research & Clinical Pharmacology.* **2019**;30:1296–1300.
- [40] Livak KJ, Schmittgen TD. Analysis of relative gene expression data using real-time quantitative PCR and the 2(-Delta Delta C(T)) method. *Methods.* **2001**;25(4):402–408.
- [41] Chen WC, Park TS, Murray IR, et al. Cellular kinetics of perivascular MSC precursors. *Stem Cells Int.* **2013**;2013:983059.
- [42] Gadelkarim M, Abushouk AI, Ghanem E, et al. Adipose-derived stem cells: effectiveness and advances in delivery in diabetic wound healing. *Biomed Pharmacother.* **2018**;107:625–633.
- [43] Veriter S, Andre W, Aouassar N, et al. Human adipose-derived mesenchymal stem cells in cell therapy: safety and feasibility in different “hospital exemption” clinical applications. *PLoS One.* **2015**;10(10):e0139566.
- [44] Mazini L, Rochette L, Admou B, et al. Hopes and limits of Adipose-Derived Stem Cells (ADSCs) and Mesenchymal Stem Cells (MSCs) in wound healing. *Int J Mol Sci.* **2020**;21(4):1306.
- [45] Xie WQ, Zhao YJ, Li F, et al. Velvet antler polypeptide partially rescue facet joint osteoarthritis-like phenotype in adult β -catenin conditional activation mice. *BMC Complement Altern Med.* **2019**;19(1):191.
- [46] Zha E, Dandan L, Bai X, et al. A recombinant polypeptide from velvet antler of *Cervus nippon* Temminck exhibits similar immunomodulatory effects as its natural counterpart. *Immunopharmacol Immunotoxicol.* **2016**;38(6):385–389.
- [47] Wang J, Wu M. The up-regulation of miR-21 by gastrodin to promote the angiogenesis ability of human umbilical vein endothelial cells by activating the signaling pathway of PI3K/Akt. *Bioengineered.* **2021**;12(1):5402–5410.
- [48] Stellavato A, Cimini D, Finamore R, et al. In vitro model based on human keratinocyte to evaluate relaxin activity on wound healing exploiting time-lapse video microscopy. *Italian Journal of Anatomy and Embryology = Archivio Italiano Di Anatomia Ed Embriologia.* **2013**;118:71–73.
- [49] Seo E, Lim JS, Jun JB, et al. Exendin-4 in combination with adipose-derived stem cells promotes angiogenesis and improves diabetic wound healing. *J Transl Med.* **2017**;15(1):35.
- [50] Tonnesen MG, Feng X, Clark RA. Angiogenesis in wound healing. *The Journal of Investigative Dermatology Symposium Proceedings.* **2000**;5(1):40–46.
- [51] Ramjiawan RR, Griffioen AW, Duda DG. Anti-angiogenesis for cancer revisited: is there a role for

- combinations with immunotherapy? *Angiogenesis*. 2017;20(2):185–204.
- [52] Lee SH, Jin SY, Song JS, et al. Paracrine effects of adipose-derived stem cells on keratinocytes and dermal fibroblasts. *Ann Dermatol*. 2012;24(2):136–143.
- [53] Beck LS, Deguzman L, Lee WP, et al. TGF-beta 1 accelerates wound healing: reversal of steroid-impaired healing in rats and rabbits. *Growth Factors*. 1991;5:295–304.
- [54] Grunewald M, Avraham I, Dor Y, et al. VEGF-induced adult neovascularization: recruitment, retention, and role of accessory cells. *Cell*. 2006;124(1):175–189.
- [55] Shen T, Pan ZG, Zhou X, et al. Accelerated healing of diabetic wound using artificial dermis constructed with adipose stem cells and poly (L-glutamic acid)/chitosan scaffold. *Chin Med J (Engl)*. 2013;126:1498–1503.
- [56] Guo R, Chai L, Chen L, et al. Stromal cell-derived factor 1 (SDF-1) accelerated skin wound healing by promoting the migration and proliferation of epidermal stem cells. *Vitro Cellular & Developmental Biology Animal*. 2015;51(6):578–585.
- [57] Zhao R, Liang H, Clarke E, et al. Inflammation in chronic wounds. *Int J Mol Sci*. 2016;17(12):2085.